

Supplementary Information for

Single-molecule imaging of the transcription factor serum response factor (SRF) reveals prolonged chromatin-binding kinetics upon cell stimulation

Lisa Hipp, Judith Beer, Oliver Kuchler, Matthias Reisser, Daniela Sinske, Jens Michaelis*, J. Christof M. Gebhardt* and Bernd Knöll*

Jens Michaelis:
jens.michaelis@uni-ulm.de

Christof Gebhardt:
christof.gebhardt@uni-ulm.de

Bernd Knöll
bernd.knoell@uni-ulm.de

This PDF file includes:

Supplementary text
Figs. S1 to S4
Table S1 and S2
Captions for movies S1 to S5
References for SI reference citations

Other supplementary materials for this manuscript include the following:

Movies S1 to S5

Supplemental Materials & Methods

Cell culture

3T3 Halo-SRF or SRF α 1 helix cells were cultured in DMEM (Dulbecco's modified Eagle's medium with GlutaMAX, Gibco) supplemented with 10% heat-inactivated Fetal Calf Serum (FCS). 100 units/mL Penicillin and Streptomycin (Pen/Strep) were added to the medium in all experiments. Halo-SRF localization was assessed by incubating with 2.5 nM TMR HaloTag ligand (Promega) in DMEM/10% FCS for 15 min at 37°C/5% CO₂ followed by extensive PBS washes according to the HaloTag protocol (Promega). Cells were fixed for 15 min in 4% PFA/5% Sucrose/PBS at RT and mounted coverslips were imaged with a Zeiss Axiovert 200M fluorescence microscope.

For cell stimulation experiments, cells were starved o/N in DMEM/0.05% FCS and stimulated with phenol red-free OptiMEM (Reduced Serum Medium, Gibco)/10% FCS for indicated time periods.

For inhibitor experiments, cells were pretreated with 10 μ M U0126 (Cell signaling) for 30 min in DMEM/0.05% FCS and stimulated with 10 μ M U0126 in OptiMEM/10% FCS for 1 h. For inhibiting F-actin polymerization, cells were pre-incubated with 0.3 μ M Latrunculin B toxin (LatB; Calbiochem) for 10 min only to ensure cell vitality.

Down-regulation of MRTF-A and MRTF-B via siRNA was realized with ON-TARGETplus SMARTpool siRNA (Dharmacon; L-054350-00-0005 and L-054677-00-0005, respectively). AllStars Negative Control siRNA (Qiagen) was used as a control. All siRNAs were delivered into cells via Lipofectamine 2000

(Invitrogen) transfection in OptiMEM at 25 nM final concentration. After 6 h, OptiMEM was replaced by DMEM/10% FCS and cells were kept two days in culture prior to starvation.

Primary hippocampal cell cultures were prepared from P1-P2 mice as previously described (1). To measure SRF binding dynamics, 0.5×10^6 cells were electroporated with 1 μg pLV-TetO-Halo-Srf construct in 100 μL Ingenio nucleofection solution (Mirus). Mock cells were electroporated with the corresponding amount of ddH₂O. For qPCR, cells were plated on 10 $\mu\text{g}/\text{mL}$ poly-L-lysine (PLL) and 2 $\mu\text{g}/\text{mL}$ laminin coated wells of a 6-well plate. For imaging experiments, glass coverslips or ΔT culture dishes (Biotechs) were coated with 100 $\mu\text{g}/\text{mL}$ PLL and 5 $\mu\text{g}/\text{mL}$ laminin. Cells were cultivated for 3 days in vitro (3 div) in NMEM/B27 neuronal culture medium with 5 $\mu\text{g}/\text{mL}$ gentamycin at 37°C/5% CO₂. For cell stimulation, neurons were incubated with 10 ng/mL brain-derived neurotropic factor (BDNF, PeproTech) in neuronal culture medium for up to 1 h at 37°C/5% CO₂.

Western blot

Protein lysates of NIH3T3 Halo-SRF cells and primary hippocampal neurons were prepared with the ISOLATE II RNA/DNA/protein kit (Bioline) according to manufacturer's instructions. 1 x PhosStop (Roche) was added to the lysates. Samples were resolved on 8-10% SDS-PAGE, followed by transfer on PVDF membranes (Amersham). After 1 h of blocking, first antibodies were applied overnight at 4°C: rabbit anti-HALO (1:1000, Promega) and rat anti-SRF (1:500,

kindly provided by A. Nordheim, Tübingen University, Germany). First antibodies were detected by horseradish-peroxidase conjugated secondary antibodies (1:2000; Santa Cruz) and the ECL Western Blotting Substrate (Pierce or Millipore).

Immunofluorescence

Cells were fixed for 15 min in 4% PFA/5% sucrose/PBS, permeabilized for 5 min in 0.1% Triton-X-100/PBS and blocked for 30 min in 2% BSA/PBS. For dSTORM imaging EM grade PFA was used (Electron Microscopy Sciences). Primary antibodies were applied overnight at 4°C: rabbit anti-HALO (1:500, Promega), rabbit anti-MRTF-A (1:1000, kindly provided by G. Posern, Halle University Clinic, Germany), goat anti-MRTF-B (1:250, Santa Cruz), rat anti-SRF (1:50, kindly provided by A. Nordheim, Tübingen University, Germany) and mouse anti β III-Tubulin (1:2000; Covance). Primary antibodies were detected with Alexa-488, Alexa-532, Alexa-647 (dSTORM) and Alexa-660 conjugated secondary antibodies (1:1500, Molecular Probes). For quantification of total SRF levels in hippocampal neurons (Fig. 6), cells were electroporated with the Halo-SRF construct and Halo-SRF was stained with TMR as described above. Fixed cells were stained for SRF with rat anti-SRF (labeling endogenous SRF and Halo-SRF) and the neuron marker β III-Tubulin. SRF signal intensity was measured at constant exposure time for TMR-positive and TMR-negative cells and determined with the Axiovision Software (Zeiss). Neurons with highest Halo-SRF overexpression exceeding the saturation limit were excluded from analysis of

total SRF levels as well as from SMT, since tracking of individual molecules was not possible.

Direct Stochastic Optical Reconstruction Microscopy (dSTORM) imaging

Immediately before imaging, fixed cells were placed in a degassed PBS imaging buffer containing 100 U/mL glucose oxidase, 400 U/mL catalase, 4% (wt/vol) glucose and 100 mM cysteamine (all from Sigma-Aldrich) at pH 7.5. Super-resolution 2D dSTORM images were acquired with a home built microscope as described in Schoen et al. (2). We analyzed images with the ImageJ plug-in ThunderSTORM (3).

Data analysis

SMT movies were analyzed by custom-written Matlab and IGOR programs to identify and track single molecules as described in (4). In short, molecules were detected at a threshold of 3.5-4 x SD over the background and positions were determined by a 2D Gaussian fit.

The bound fraction was determined as described in Speil et al. (5). Briefly, we calculated the displacement of moving and bound molecules between two consecutive 10 ms frames. The cumulative distribution of the resulting diffusion coefficients was globally fitted by a three-component diffusion model:

$$F\left(\frac{x^2 + y^2}{4\tau}\right) = A_1\left(1 - \exp\left(-\frac{x^2 + y^2}{4D_1\tau}\right)\right) + A_2\left(1 - \exp\left(-\frac{x^2 + y^2}{4D_2\tau}\right)\right) \\ + (1 - A_1 - A_2)\left(1 - \exp\left(-\frac{x^2 + y^2}{4D_3\tau}\right)\right)$$

(Eq. I)

where A_1 , A_2 and $(1 - A_1 - A_2)$ are the amplitudes of the diffusion coefficients D_1 , D_2 and D_3 . The amplitude of the slowest diffusion coefficient caused by the localization error of detected bound molecules corresponds to the fraction of bound molecules. To avoid crossing of paths, we set an upper limit of 8 pixels for the maximum squared displacement and replaced the last term of equation I by:

$$(1 - A_1 - A_2)\left(\exp\left(-\frac{x^2 + y^2}{4D_3\tau}\right) - 1\right) / \left(\exp\left(-\frac{C}{D_3}\right) - 1\right)$$

(Eq. II)

where C is the constant denoting the upper limit for the squared displacement of 8 pixels.

We globally fitted the diffusion coefficients for all conditions, whereas amplitudes were fitted individually for each condition. Values and errors for all fractions were calculated by bootstrapping, where mean \pm SEM for each dataset were obtained from global fits to 2.000 random subsets of displacements, each consisting of 80% of the original data.

Chromatin residence times were determined as described in (4). To distinguish between dissociation events and photobleaching of fluorophores we extracted binding events from continuous and time-lapse movies. Molecules present in two consecutive frames within 1-2 pixels depending on the time-lapse time were

regarded as bound. Histograms of fluorescent 'on' times were globally fitted with a Levenberg-Marquardt least squares algorithm in Igor Pro (WaveMetrics, Portland, USA) using decay models including a photobleaching rate constant (k_b) and varying numbers of dissociation rate constants (k_{off}). Reduced chi-squared analysis revealed that data extracted from fibroblasts as well as hippocampal neurons is best characterized by a model including three dissociation rate constants:

$$\begin{aligned}
 f_T(t) = & A \cdot \left[B \cdot \left(k_b \cdot \left(\frac{\tau_{int}}{\tau_{tl}} \right) + k_{off,1} \right) \cdot \exp \left(- \left[k_b \cdot \left(\frac{\tau_{int}}{\tau_{tl}} \right) + k_{off,1} \right] \cdot t \right) \right. \\
 & + C \cdot \left(k_b \cdot \left(\frac{\tau_{int}}{\tau_{tl}} \right) + k_{off,2} \right) \cdot \exp \left(- \left[k_b \cdot \left(\frac{\tau_{int}}{\tau_{tl}} \right) + k_{off,2} \right] \cdot t \right) \\
 & \left. + (1 - B - C) \cdot \left(k_b \cdot \left(\frac{\tau_{int}}{\tau_{tl}} \right) + k_{off,3} \right) \cdot \exp \left(- \left[k_b \cdot \left(\frac{\tau_{int}}{\tau_{tl}} \right) + k_{off,3} \right] \cdot t \right) \right]
 \end{aligned}$$

(Eq. III)

$f_T(t)$ represents the probability density of dissociation times. The amplitude A , the photobleaching constant k_b , the off-rate constants k_{off1} , k_{off2} , k_{off3} and the fractions B and C were optimized during the fit. k_b and k_{off1} were globally fitted using data from unstimulated, 1 h and 2 h stimulated cells (Fig. 3), from DMSO, U0126 and LatB-treated cells (Fig. 5) as well as from unstimulated and BDNF-stimulated neurons (Fig. 6).

Supplementary Figures

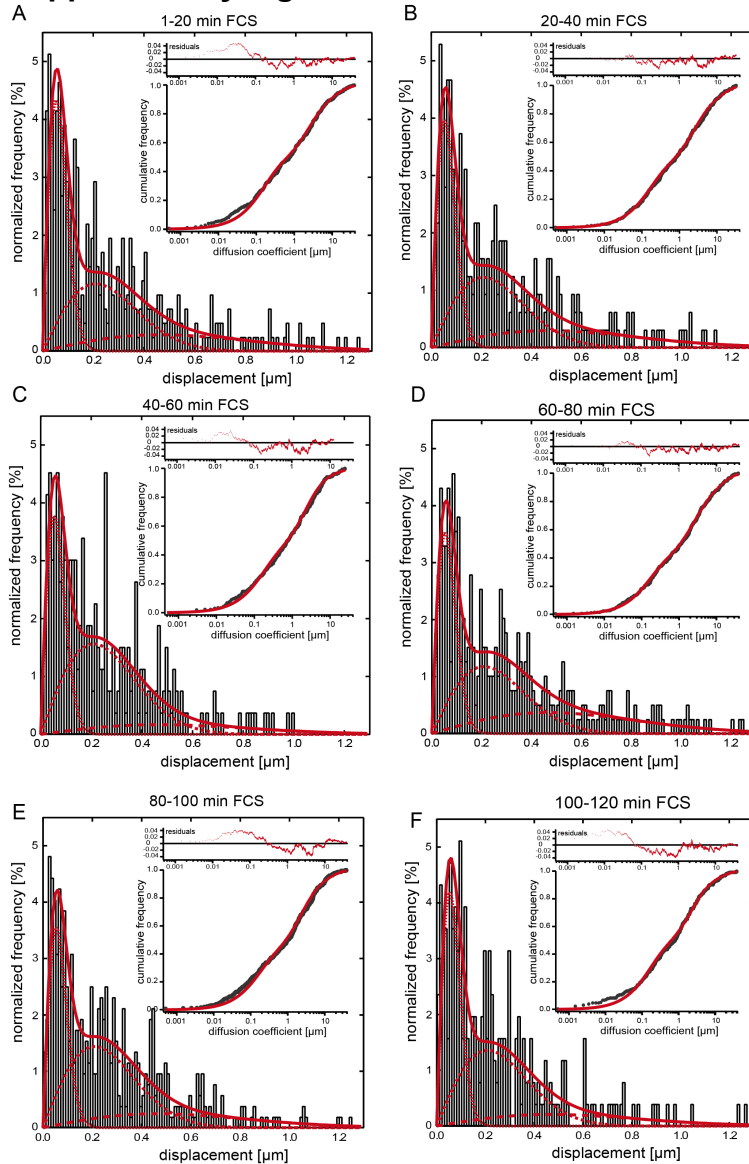


Fig. S1

Displacement histograms for all conditions involving FCS stimulation

Histograms of displacements for all stimulation time windows after FCS application in NIH3T3 cells (1-20 min: N = 409 molecules, N = 9 cells; 20-40 min: N = 321 molecules, N = 9 cells; 40-60 min: N = 265 molecules, N = 8 cells; 60-80 min: N = 394 molecules, N = 7 cells; 80-100 min: N = 519 molecules, N = 9 cells; 100-120 min: N = 254 molecules, N = 7 cells). The distributions were fitted with a three-component diffusion model (equation I, II in methods) where the lowest diffusion component is representative of chromatin-bound molecules. The inset shows the residuals (red dots, upper insert) from the three-component fit (red line, lower part of insert) to the cumulative distribution of the calculated squared displacements per 10ms integration time for a two-dimensional diffusion (in black) for all conditions

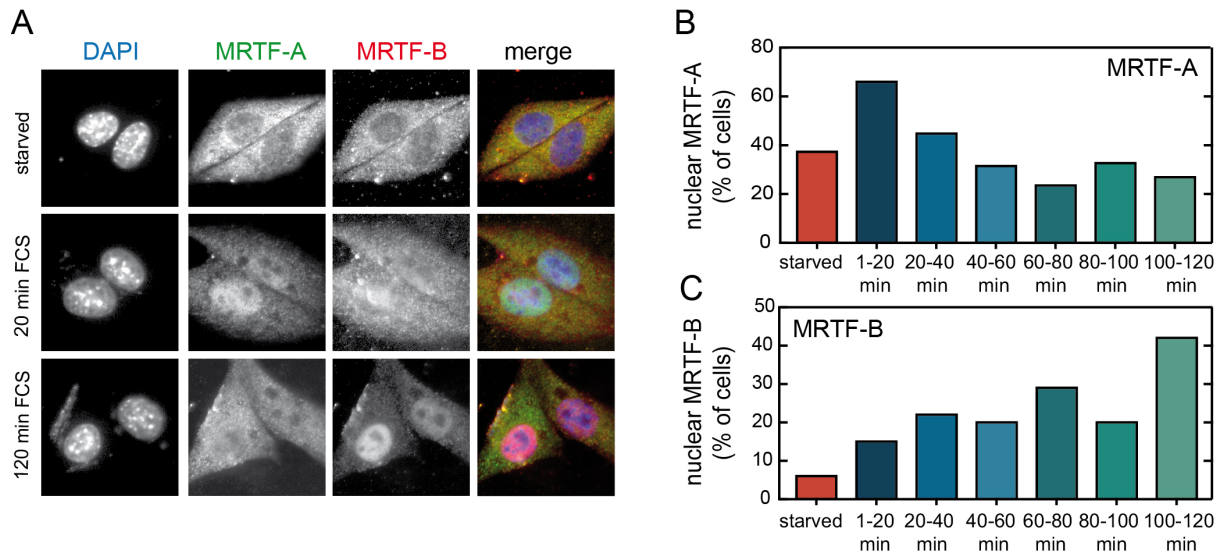


Fig. S2

FCS stimulates nuclear entry of SRF co-factors MRTF-A and MRTF-B

A NIH3T3 cells were stimulated with 10% FCS for 20 or 120 minutes. Subsequently, cells were stained for MRTF-A (green) or MRTF-B (red) localization.

B, C MRTF-A (B) nuclear localization increased at 20 minutes after stimulation whereas MRTF-B (C) accumulated in the nucleus at later timepoints.

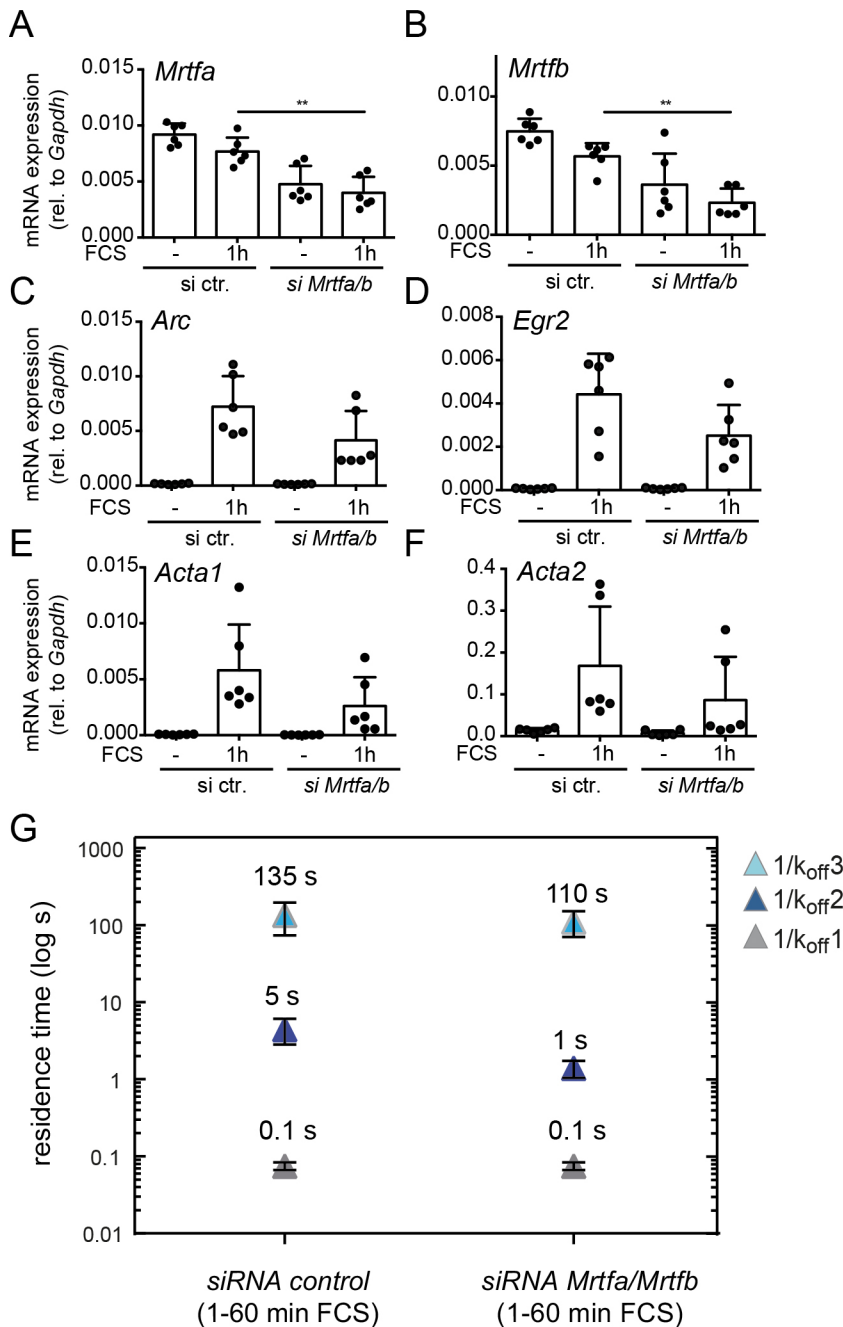


Fig. S3

siRNA mediated *Mrtfa/Mrtfb* depletion interferes with SRF residence time

A, B siRNA directed against *Mrtfa* and *Mrtfb* reduced mRNA abundance of both genes.

C-F Upon *Mrtf* depletion, SRF target gene abundance of *Arc* (C), *Egr2* (D), *Acta1* (E) and *Acta2* (F) is reduced. Data is depicted as mean \pm SD (** $p \leq 0.01$, Mann-Whitney U test).

G *siMrtfa/Mrtfb* reduced SRF residence times compared to control siRNA. Both, the long bound and intermediate bound SRF residence times were decreased.

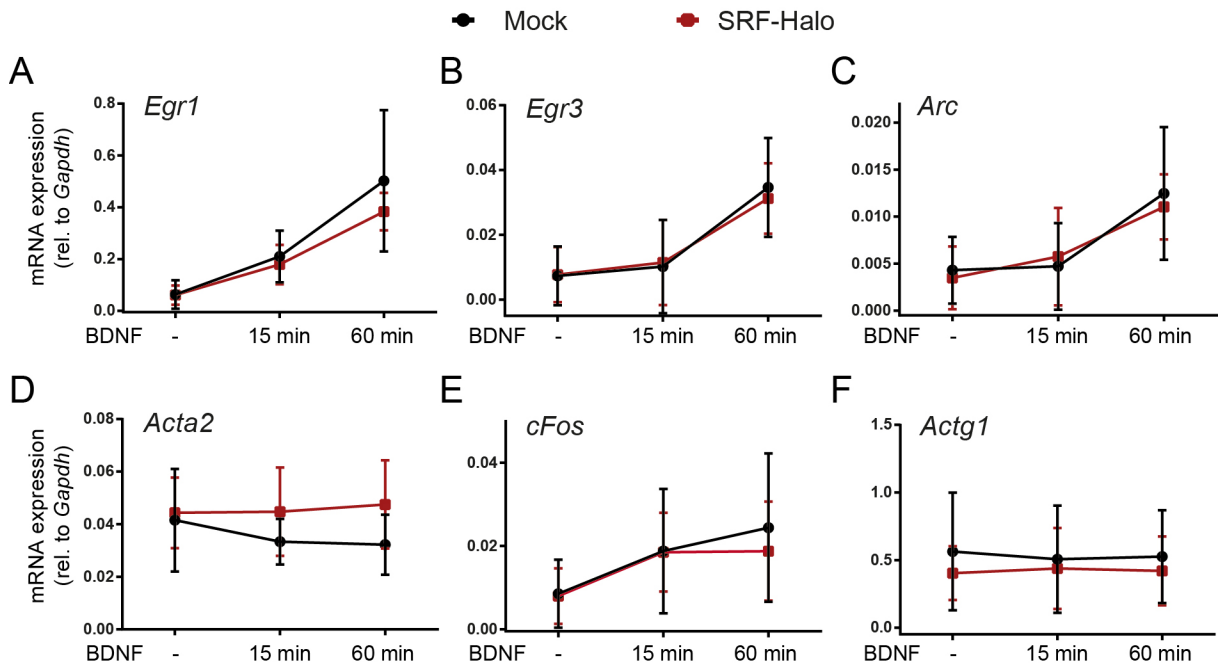


Fig. S4

Gene induction of SRF target genes in primary neurons

A-F Primary hippocampal neurons expressing Halo-SRF or endogenous SRF only (mock) were stimulated with BDNF for 15 or 60 minutes. Subsequently, cDNA was subjected to qPCR analysis with primers indicated.

IEG encoding genes *Egr1* (A), *Egr3* (B), *Arc* (C) and *cFos* (E) were up-regulated by BDNF in a similar manner in mock (black lines) and Halo-SRF (red lines) expressing cells. In contrast, both cytoskeletal genes, *Acta2* (D) and *Actg1* (F), were not induced by BDNF.

Supplementary Tables

Table S1
Primer sequences

Primer	Sequence
Acta1 (fw)	5' -TAC CAC CGG CAT CGT GTT - 3'
Acta1 (rv)	5' -CAG GTC CAG ACG CAT GAT GG - 3'
Acta2 (fw)	5'- CAG CAA ACA GGA ATA CGA CGA A- 3'
Acta2 (rv)	5'- TGT GTG CTA GAG GCA GAG CAG - 3'
Actg1 (fw)	5' -CAA GAA ATG GCT ACT GCT GCA T - 3'
Actg1 (rv)	5' -ACT CCA TGC CCA GGA AGG AA - 3'
Ankrd1 (fw)	5' - GGA TGT GCC GAG GTT TCT GA - 3'
Ankrd1 (rv)	5' - AGT GCC GTC CGT TTA TAC TCA - 3'
Arc (fw)	5' - GCA CAA AAG CCA TGA CCC AT - 3'
Arc (rv)	5' - TCT CCC TAG TCC CCA GGG C - 3'
cFos (fw)	5' - CCT GCC CCT TCT CAA CGA C - 3'
cFos (rv)	5' - GCT CCA CGT TGC TGA TGC T - 3'
Egr1 (fw)	5' - GCC GAG CGA ACA ACC CTA T - 3'
Egr1 (rv)	5' -TCC ACC ATC GCC TTC TCA TT - 3'
Egr3 (fw)	5' - GAG ATC CCC AGC GCG - 3'
Egr3 (rv)	5' - CAT CTG AGT GTA ATG GGC TAC CG - 3'
Gapdh (fw)	5' - TGG ATC TGA CGT GCC GC - 3'
Gapdh (rv)	5' - TGC CTG CTT CAC CAC CTT C - 3'
Mrtf-A (fw)	5' - TAG TGA GCG GAA GAA TGT GC - 3'
Mrtf-A (rv)	5' - ATC CCT TGG CTC ACC AGT T - 3'
Mrtf-B (fw)	5' - TCC AGA GGT TTC CAG TGT GC - 3'
Mrtf-B (rv)	5' - ATG CTG GCT GTC ACT GGT TT - 3'
Tpm1α (fw)	5' - CTG ATA AGA AGG CGG CGG - 3'
Tpm1α (rv)	5' - TCT TTT GCA GTG ACA CCA GCT C - 3'
Acta2 (fw) ChIP	5'- GGA GCA GAA CAG AGG AAT GCA- 3'
Acta2 (rv) ChIP	5'- GCT TCC CAA ACA AGG AGC AA- 3'
Ankrd1 (fw) ChIP	5' - ACC TAC AGT CTC TTC CAA ACC ATG T - 3'
Ankrd1 (rv) ChIP	5' - CCA GTG AGC AGA GCA ATT TCC - 3'
cFos (fw) ChIP	5' - TCC CTC CCT CCT TTA CAC AG - 3'
cFos (rv) ChIP	5' - GTG TAG GAT TTC GGA GAT GGT C - 3'
Egr1 (fw) ChIP	5' - CCC ACC ACT CTT GGA TGG GAG GGC TTC AC - 3'
Egr1 (rv) ChIP	5' - TCG GCC TCT ATT TCA AGG GTC TGG AAC AGC - 3'

Table S2
Summary table comparing different parameters in fibroblasts and primary neurons.

embryonic fibroblast				hippocampal neuron		
diff. coeff.	starved and stimulated (pooled)					
bound	$D_1 = 0.14 \pm 0.02 \mu\text{m}^2/\text{s}$			n.d.		
slow diffusing	$D_2 = 2.18 \pm 0.40 \mu\text{m}^2/\text{s}$					
fast diffusing	$D_3 = 10.8 \pm 2.23 \mu\text{m}^2/\text{s}$					
fractions	starved	1-20 min FCS				
bound	35.4 ± 2.8 %	38.4 ± 3.9 %		n.d.		
slow diffusing	39.9 ± 5.5 %	42.1 ± 6.3 %				
fast diffusing	21.7 ± 4.8 %	22.9 ± 5.8 %				
long bound fraction	starved	1-20 min FCS		starved	1-20 min FCS	
	17.4 ± 4.9 %	24.8 ± 6.4 %		27.1 ± 2.1 %	36.3 ± 2.7 %	
res. time	starved	1-60 min	60-120 min	starved	1-60 min	60-120 min
long bound	55 ± 20 s	278 ± 177 s	145 ± 74 s	10 ± 2 s	27 ± 5 s	
inter. bound	3 ± 1 s	4 ± 1 s	9 ± 2 s	1.4 ± 0.3 s	0.9 ± 0.2 s	n.d.
short bound	0.1 ± 0.01 s	0.1 ± 0.01 s	0.1 ± 0.01 s	0.1 ± 0.01 s	0.1 ± 0.01 s	
global fit	three-rate			three-rate		

Captions for movies S1 to S5

Movie S1

Live cell imaging of a NIH3T3 cell transfected with Halo-SRF showing immobilized and highly mobile Halo-SRF molecules. 2 x 10 ms exposure times were interspersed with 5 s dark time. The dark time was shortened to 0.5 s for convenience. Please note that some molecules move a certain distance in the focus plane between the two illuminations. In addition, some molecules move out of the focus plane (in z-direction) thereby disappearing after the first illumination.

Movie S2

A NIH3T3 cell transfected with Halo-SRF was stimulated with 10% FCS to determine the SRF residence time. The movie depicts individual Halo-SRF molecules in the nucleus. Several SRF molecules remaining at the same position over several frames are visible indicating chromatin association. A 50 ms integration time was interspersed with 100 ms timelapse time.

Movie S3

A NIH3T3 cell expressing Halo-SRF was imaged with the ITM protocol to identify long-bound SRF molecules associating with chromatin for at least two seconds. Here, 2x 50 ms exposures were followed by a 2s timelapse.

Movie S4

A living primary mouse hippocampal neuron expressing individual Halo-SRF molecules was imaged. In the nucleus of this cell several Halo-SRF molecules associated with chromatin. A 50 ms integration time was interspersed with 100 ms timelapse time.

Movie S5

The nucleus of a primary hippocampal neuron expressing Halo-SRF was recorded with the ITM protocol. Several long-bound chromatin associated SRF molecules are visible. In ITM, 2x 50 ms exposures were followed by a 2s timelapse.

Supplementary References

1. Knoll B, *et al.* (2006) Serum response factor controls neuronal circuit assembly in the hippocampus. *Nature neuroscience* 9(2):195-204.
2. Schoen M, *et al.* (2015) Super-Resolution Microscopy Reveals Presynaptic Localization of the ALS/FTD Related Protein FUS in Hippocampal Neurons. *Frontiers in cellular neuroscience* 9:496.
3. Ovesny M, Krizek P, Borkovec J, Svindrych Z, & Hagen GM (2014) ThunderSTORM: a comprehensive ImageJ plug-in for PALM and STORM data analysis and super-resolution imaging. *Bioinformatics* 30(16):2389-2390.
4. Gebhardt JC, *et al.* (2013) Single-molecule imaging of transcription factor binding to DNA in live mammalian cells. *Nature methods* 10(5):421-426.
5. Speil J, *et al.* (2011) Activated STAT1 transcription factors conduct distinct saltatory movements in the cell nucleus. *Biophysical journal* 101(11):2592-2600.